Dissipative Particle Dynamics Simulation for Vesicle Shape Change

Yoshiyuki Oofuji[1], Naohito Urakami[1], Masayuki Imai[2], Takashi Yamamoto[1]

[1]*Department of Physics and Information Sciences, Yamaguchi University, Yamaguchi 753-8512, Japan*
[2]*Department of Physics, Tohoku University, Sendai 980-8578*
Tel: 81-83-933-5690; Fax: 81-83-933-5690
urakami@yamaguchi-u.ac.jp

Abstract: Spherical vesicles can change to various shapes such as oblate, prolate, stomatocyte-like, and starfish-like, according to the osmotic pressure difference between the inner and outer vesicles. The shape changes of vesicles are very important for understanding the activities of living cells. In this study, we investigated the process of vesicle shape change by carrying out dissipative particle dynamics simulations. We prepared spherical vesicles in which the difference between the numbers of lipids forming the inner and outer leaflets (ΔN) varied. If ΔN was small, with a decrease in the number of water beads inside a vesicle (N_w), a transformation from sphere to oblate, then oblate to stomatocyte-like was observed. If ΔN was large, a transformation from sphere to prolate, then prolate to tube-like occurred. The vesicles shape changes were in good agreement with the experiments. To investigate the mechanism of vesicle transformation in detail, we performed simulations by moving lipids between the inner and outer vesicle leaflets to vary ΔN. As a result, a transformation between the prolate and oblate vesicles was observed. These results indicated that the shapes of vesicles were determined by ΔN and N_w.

Keywords: Vesicle Shape Change, Biomembrane, Dissipative Particle Simulation, Area Difference Model

I. INTRODUCTION

Lipid molecules are the main constituent of biomembranes, and they can self-assemble into various types of structures such as micelles, cylinders, and bilayers (lamellae or vesicles) in an aqueous solution. Vesicles have a closed surface with a bilayer structure, and they have been used as a model system of biomembranes in many experiments designed to investigate the various phenomena observed in living cells, such as the formation of lipid domains [1-4] on the membrane and the diffusion of lipids [5] in the membrane. In addition, the vesicle is a strong candidate for the transport of drug components across the cell membrane, and it plays an important role in cosmetic and food materials.

One of the fascinating properties of lipid membranes is that they form various shapes; they may be spherical, prolate, oblate, stomatocyte-like, starfish-like, etc. [6-8]. Moreover, the vesicles change their shape according to external stimuli. For example, depending on the osmotic pressure difference between the inner and outer vesicles, the water molecules move from the inside to the outside, and a spherical vesicle thus becomes oblate or prolate. With further reduction in the internal volume of the vesicle, an oblate vesicle becomes shaped like a stomatocyte or starfish. In contrast, a prolate vesicle changes shape to a tube or pear [6, 7]. In this way, the vesicles transform to various shapes.

The area difference elasticity (ADE) model [9] has been suggested as a means of understanding the various shapes of vesicles. The ADE model introduces two important parameters: an excess area and an intrinsic area difference. The excess area is the area-to-volume ratio, and the intrinsic area difference is determined by the number of lipids in the outer and inner leaflets. The vesicle shapes are determined by minimizing the sum of the bending energy of the membrane and the energy resulting from the intrinsic area difference, and various vesicle shapes were interpreted on the basis of the ADE model. However, it is difficult to compare the theoretical results with the experimental results because of the difficulty in counting the number of lipids in the two leaflets.

Such difficulty motivated computational studies of vesicles. In the past decade, many computational studies on vesicles have been reported. For instance, vesicle formation from random state [10], formation of lipid domains and budding process [11, 12], and fusion and fission of vesicles [13] have been reported using dissipative particle dynamics (DPD) simulations [14, 15]. In addition, the vesicle shapes consisting of triblock copolymers [16] and the transformation of vesicle shapes in small systems [17] were investigated by DPD simulations. Therefore, DPD simulation is an efficient method of investigating the shape changes of vesicles.

In this work, we carried out DPD simulations to reproduce the various shapes of vesicles observed in the experiment. The transformation of vesicles from a

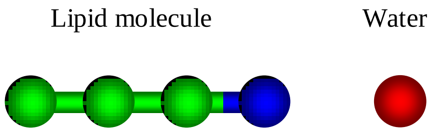

Fig. 1 Illustrations of coarse-grained models used in our simulation. The lipid molecule is represented by one hydrophilic head bead (H) and three hydrophobic tail beads (T). The water molecule is represented by a single hydrophilic bead (W).

spherical shape that accompanied a decrease in the internal volume of the vesicle was investigated. Moreover, the transformation of vesicles induced by the flip-flop of lipids between the outer and inner leaflets was also explored.

II. SIMULATION MODELS AND METHODS

We used coarse-grained models for lipids and water molecules. As shown in Fig. 1, the lipids were represented by one hydrophilic head bead (H) and three hydrophobic tail beads (T), and the water molecules were represented by a single hydrophilic bead (W). All beads have the same mass m. The numbers of lipid and water molecules were 10,000 and 400,000, respectively.

In the DPD simulation, the position and velocity of each bead i are denoted by $(\boldsymbol{r}_i, \boldsymbol{v}_i)$. The time evolution is governed by Newton's equation of motion. The forces acting between the i-th and j-th beads are a conservative force $\boldsymbol{F}_{ij}^{(\mathrm{C})}$, a dissipative force $\boldsymbol{F}_{ij}^{(\mathrm{D})}$, and a pairwise random force $\boldsymbol{F}_{ij}^{(\mathrm{R})}$. These three forces are given as follows:

$$\begin{aligned} \boldsymbol{F}_{ij}^{(\mathrm{C})} &= a_{ij}\omega(r_{ij})\hat{\boldsymbol{r}}_{ij}, \\ \boldsymbol{F}_{ij}^{(\mathrm{D})} &= -\gamma\omega^2(r_{ij})(\hat{\boldsymbol{r}}_{ij}\cdot\boldsymbol{v}_{ij})\hat{\boldsymbol{r}}_{ij}, \\ \boldsymbol{F}_{ij}^{(\mathrm{R})} &= \sigma\omega(r_{ij})\theta_{ij}(t)\hat{\boldsymbol{r}}_{ij}, \end{aligned} \tag{1}$$

where a_{ij} is the maximum repulsion force between i-th and j-th beads, $\hat{\boldsymbol{r}}_{ij} = \boldsymbol{r}_{ij}/r_{ij}$, $\boldsymbol{r}_{ij} = \boldsymbol{r}_i - \boldsymbol{r}_j$, $r_{ij} = |\boldsymbol{r}_{ij}|$, and $\boldsymbol{v}_{ij} = \boldsymbol{v}_i - \boldsymbol{v}_j$. The parameters γ and σ are related to each other by the fluctuation-dissipative theorem:

$$\sigma^2 = 2\gamma k_{\mathrm{B}}T, \tag{2}$$

where k_{B} and T are the Boltzmann constant and the thermostat temperature, respectively. The weight function $\omega(r)$ is chosen as follows:

$$\omega(r) = \begin{cases} 1 - r/r_0 & r \le r_0 \\ 0 & r > r_0 \end{cases} \tag{3}$$

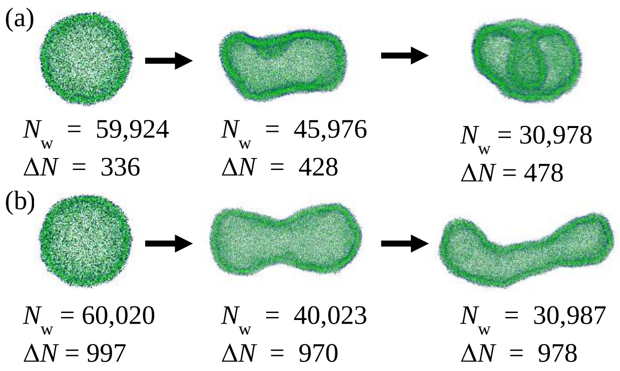

Fig. 2 Shape changes from spherical vesicles, with a decrease in the number of water beads in vesicles. In the initial spherical vesicles, (a) (N_{w}; ΔN) = (59,924; 336) and (b) (60,020; 997). Water beads are not displayed for clarity.

where r_0 is the cutoff radius, and $\theta_{ij}(t)$ is a random variable satisfying the following:

$$\begin{aligned} &\langle \theta_{ij}(t) \rangle = 0 \\ &\langle \theta_{ij}(t)\theta_{kl}(t') \rangle = (\delta_{ik}\delta_{jl} + \delta_{il}\delta_{jk})\delta(t - t'). \end{aligned} \tag{4}$$

The spring force for lipids is given by the equation:

$$\boldsymbol{F}_{ij}^{(\mathrm{S})} = -C(1 - r_{i,i+1}/b)\hat{\boldsymbol{r}}_{i,i+1} \tag{5}$$

where $r_{i,i+1}$ denotes the distance between connected beads, b is the equilibrium bond distance, and C is the force constant.

The parameters a_{ij} was set to 25ε for between hydrophilic beads (H and W) and for between hydrophobic beads (T), where ε is the energy unit. For between hydrophilic and hydrophobic beads, a_{ij} was set to 200ε. The noise parameter σ was set to 3.0 and $k_{\mathrm{B}}T$ = ε. In the spring force, C = 100ε and b = $0.45r_0$. The number density was $3.0r_0^{-3}$. For the other simulation parameters, the same parameters as in the reference [12] were used. Our simulations were carried out using the COGNAC within the OCTA program [18].

In our simulations, in order to investigate the shape changes of vesicles, we varied two parameters: the number of water beads inside a vesicle, N_{w}, and the difference between the number of lipids, $\Delta N = N_{\mathrm{out}} - N_{\mathrm{in}}$, where N_{out} and N_{in} denoted the number of lipids in the outer and inner leaflet of a vesicle, respectively. The parameters N_{w} and ΔN correspond to the excess area and the intrinsic area difference in the ADE model. N_{w} was reduced by moving the water beads inside a vesicle to the outside, and ΔN was varied by the flip-flop of the lipids between the inner and outer leaflets.

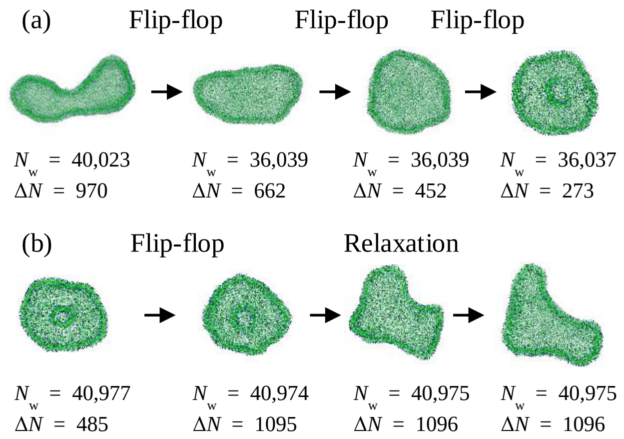

Fig. 3 Transformation of vesicle shapes by changing ΔN. (a) Tube-like vesicle transforms to stomatocyte by moving the lipids from the outer to the inner leaflets in a step-by-step manner. (b) Stomatocyte vesicle transforms to a triangular oblate shape by moving the lipids from the inner to the outer leaflets at the first step.

III. SIMULATION RESULTS

1. Transformation of vesicle shape by changing N_w

We examined the transformation of vesicle shape from spherical to the other shapes. In order to reproduce the volume change of a vesicle in our simulations, 1,000 water beads inside a vesicle were selected randomly, and transferred outside the vesicle in every 5,000 steps. In this way, the number of water beads inside the vesicle (N_w) decreased during simulation runs. As shown in Fig. 2, we prepared two types of spherical vesicles, N_w = 59,924, ΔN = 336 and N_w = 60,020, ΔN = 997. For a small ΔN, with a decrease in N_w, the spherical vesicle became oblate at N_w = 45,976, and stomatocyte-shaped at N_w = 30,978 (Fig. 2 (a)). In contrast, for a large ΔN, with a decrease in N_w, the vesicle shape changed from spherical to prolate at N_w = 40,023, and to a tube at N_w = 30,987 (Fig. 2 (b)). The transformation sequence obtained in the simulation is in good agreement with the experiment [6, 7]. During the simulations, ΔN changed because the spontaneous flip-flop of lipids occurred. Moreover, the variation of N_w occurred because of the spontaneous transfer of water beads between the inside and outside of a vesicle. However, these variations in ΔN and N_w were small and could be neglected. Therefore, the results show that the difference in the initial structures of vesicles is important in determining which branch of transformation the sphere is subject to (oblate or prolate).

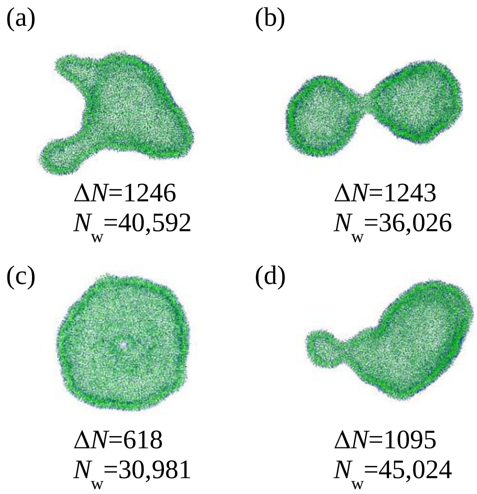

Fig. 4 Various shapes of vesicles obtained by our simulations by changing N_w and ΔN. (a) Starfish-like shape, (b) dumbbell, (c) torus, and (d) racket.

2. Transformation of vesicle shapes by changing ΔN

In order to confirm that the difference of ΔN determines vesicle shape, we investigated the shape changes caused by the flip-flop of lipids between the inner and outer leaflets. During the simulation run, the water beads were not moved from the inside to the outside vesicle but there was a spontaneous transfer of water beads, so N_w was kept almost constant. As shown in Fig. 3(a), the lipids in the tube-like vesicle were moved from the outer to the inner leaflets, that is, ΔN changed from 970 to 273 in a step-by-step manner. The tube-like vesicle became oblate and stomatocyte-shaped. In the stomatocyte vesicle in Fig. 3(b), the lipids moved from the inner to the outer leaflets, and ΔN changed from 485 to 1096 at the first step. In fact, the stomatocyte-shaped vesicle changed to a triangular oblate shape. From the results, we concluded that the shapes of vesicles were determined by ΔN. The transformation sequences obtained in the simulations were also observed in the experiment [8], which was carried out on the condition that the volume of vesicles remained almost unchanged.

3. Various shape changes of vesicles

In the simulations, we reproduced various shape changes of vesicles resulting from changes in N_w and ΔN, as shown in Fig. 4. The starfish-like vesicle was derived from the stomatocyte vesicle by increasing ΔN. The dumbbell-like vesicle was obtained from the prolate vesicle by decreasing N_w and increasing ΔN. The oblate vesicle became torus-shaped following a decrease in N_w. The racket was obtained from a spherical vesicle by increasing ΔN. These vesicle shapes were observed in the experiments [6-8]. It was possible to reproduce the various vesicle shapes using our model for the simulations.

IV. CONCLUSION

We carried out DPD simulations to investigate the transformation of vesicle shapes from spherical to the other shapes with a decrease in N_w. For small ΔN, the vesicle changed from spherical to oblate. In contrast, for large ΔN, the vesicle changed from spherical to prolate. With further reduction in N_w, the oblate vesicle became stomatocyte-like, and the prolate vesicle changed to a tube. The results were in good agreement with the experimental results [6, 7]. To investigate the mechanism of the vesicle shape changes in detail, we carried out the simulations by moving lipids between the inner and outer leaflets of the vesicle. We observed the vesicle shape change from a tube to prolate, oblate, and finally, stomatocyte-like when lipids were moved from the outer to the inner leaflet, corresponding to a decrease in ΔN. In contrast, there was a transformation from stomatocyte-like to triangular oblate when lipids were moved from the inner to the outer leaflet, corresponding to an increase in ΔN. These results indicate that the shapes of vesicles are determined by N_w and ΔN. The vesicle shapes obtained in the simulations were comparable with those predicted by the ADE model. In addition, we also obtained the starfish, dumbbell, torus, and racket shapes by varying N_w and ΔN. In the future, we must analyze these vesicle shapes in detail, and we will clarify the mechanism of various vesicle shape changes. Information about the shape changes of vesicles would help us to understand the motion of living cells when reacting to external stimuli.

ACKNOWLEDGEMENTS

This work was supported by JSPS KAKENHI Grant Number 24540437, 25247070.

REFERENCES

[1] Veatch SL, Keller SL (2002) Organization in lipid membranes containing cholesterol. Phys. Rev. Lett., 89:268101(1-4).

[2] Veatch SL, Keller SL (2005) Miscibility phase diagrams of giant vesicles containing sphingomyelin. Phys. Rev. Lett., 94:148101(1-4).

[3] Masui T, Urakami N, Imai M (2008) Nano-meter–sized domain formation in lipid membranes observed by small angle neutron scattering. Eur. Phys. J. E, 27:379-389.

[4] Cicuta P, Keller SL, Veatch SL (2007) Diffusion of liquid domains in lipid bilayer membranes. J. Phys. Chem. B, 111:3328-3331.

[5] Scherfeld D, Kahya N, Schwille P (2003) Lipid dynamics and domain formation in model membranes composed of ternary mixtures of unsaturated and saturated phosphatidylcholines and cholesterol. Biophys. J., 85:3758-3768.

[6] Hotani H (1984) Transformation pathways of liposomes. J. Mol. Biol. 178(1):113-120.

[7] Yanagisawa M, Imai M, Taniguchi T (2008) Shape deformation of ternary vesicles coupled with phase separation. Phys. Rev. Lett. 100:148102(1-4).

[8] Sakashita A, Urakami N, Ziherl P, Imai M (2012) Three-dimensional analysis of lipid vesicle transformations. Soft Matter, 8:8569-8581.

[9] Seifert U (1997) Configurations of fluid membranes and vesicles. Adv. Phys., 46:13-137.

[10] Yamamoto S, Maruyama Y, Hyodo S (2002) Dissipative particle dynamics study of spontaneous vesicle formation of amphiphilic molecules. J. Chem. Phys., 116:5842-5849.

[11] Yamamoto S, Hyodo S (2003) Budding and fission dynamics of two-component vesicles. J. Chem. Phys., 118:7937-7943.

[12] Laradji M, Kumar PBS (2004) Dynamics of Domain Growth in self-assembled fluid vesicles. Phys. Rev. Lett., 93:198105(1-4).

[13] Granfmüller A, Shillcock J, Lipowsky R (2007) Pathway of Membrane fusion with two tension-dependent energy barriers. Phys. Rev. Lett., 98:218101(1-4).

[14] Groot RD, Warren PB (1997) Dissipative particle dynamics: Bridging the gap between atomistic and mesoscopic simulation. J. Chem. Phys., 107:4423-4435.

[15] Groot RD, Madden TJ (1998) Dynamic simulation of diblock copolymer microphase separation. J. Chem. Phys., 108:8713-8724.

[16] Li X, Pivkin IV, Liang H, Karniadakis GE (2009) Shape Transformations of membrane vesicle from amphiphilic triblock copolymer. A dissipative particle dynamics simulation study, Macromolecules, 42:3195-3200.

[17] Noguchi I, Urakami N, Imai M, Yamamoto T (2010) Simulation of shape transformations of lipid bilayer vesicles (in Japanese). Kobunshi Ronbunshu, 67:605-610.

[18] Aoyagi T, Sawa F, Shoji T, Fukunaga H, Takimoto J, Doi M, (2002) A general-purpose coarse-grained molecular dynamics program. Comput. Phys. Commun., 145:267-279.